Pseudorange Double Difference and PDR Fusion Algorithm Using Smartphone GNSS Raw Measurements

Zida Wu[1], Peilin Liu, Qiang Liu, Yuze Wang, Jiuchao Qian and Huiping Zhu

Abstract. Limited by the low-cost antenna of mobile phones and unstable crystal oscillator, the positioning accuracy of existing smartphones can only reach about 10 meters. Compared to GNSS typical shortcomings, such as weak signal, low update rate and static divergence, high update rates and independent of outside information make IMU (Inertial Measurement Unit) become an ideal fusion option. But the analysis shows that the MEMS-based IMU owes high instability and severe cumulative errors make it difficult to directly integrate with GNSS. The target of this paper is to achieve high-precision positioning by using the GNSS chip raw observation data and IMU information. Pseudorange double difference (PDD) and PDR were chosen as the fusion algorithm sub-systems. This paper analyzes the constraints of high-precision positioning of mobile phones, and then the main error sources of GNSS were eliminated by establishing a pseudorange double-difference model based on smart phones. Afterwards an error estimation model was established to induce PDR technology to correct the positioning quality in complex environments such as tunnels and tree shade, the estimator was fed back to PDR simultaneously. Ultimately, tests were carried out in various scenarios and the performance analysis of the algorithm was given. Experiments show that compared with the traditional positioning technology, PDD-PDR fusion algorithm would show obvious better positioning performance, which can achieve 5m positioning accuracy under dynamic and static alternating motion and short-time tunnel conditions.

Keywords: smartphone • sport state monitor • PDD • PDR • Integrated Navigation

Z. Wu (✉) • P. Liu • Q. Liu • Y. Wang • J. Qian • H. Zhu
School of Electronic Information and Electrical Engineering,
Shanghai Jiao Tong University, Shanghai, China
e-mail: wuzida@sjtu.edu.cn

1 Introduction

In the past few decades, the development of GNSS navigation system has greatly improved the positioning accuracy, limited by hardware conditions and cost issues, the accuracy of intelligent terminals has been hardly improved, especially for mobile phones. But there is a strong demand for high-precision positioning of intelligent terminals in life. For the mobile phone's meter-level positioning technology, it has been relying on other positioning technologies, such as Wi-Fi, Bluetooth, UWB, etc., but these positioning methods need to deploy a large number of external devices, and are mostly used for indoor positioning, it is not suitable for outdoor conditions.

The opening of Android's original observations makes high-precision positioning of the mobile phone possible, Pesyna et al. [1-3] demonstrated that antenna and the GNSS chipset through the antenna and chip externally have the ability to obtain high-precision positioning results, while [4] shows that the mobile phone is fully capable of independently achieving the Pseudorange double difference (PDD) precision. The positioning result also indicates that the GNSS signal on the mobile terminal performs extremely poorly when it encounters blocking, and the static motion state cannot be distinguished, so that the static positioning result is diverged, so a certain auxiliary technology is needed for fusion.

Compared to visual and map matching techniques, which require a certain amount of prior knowledge and large computational complexity, inertial devices that is independent of external information become an ideal choice. However, low-power MEMS has a lot of noise and random drift. It is unrealistic to use the built-in IMU of the smartphone to navigate the INS system, and the second integral operation directly with the IMU accelerometer has a very small influence on the position. Whereas, Pedestrian dead reckoning (PDR) technology can make up for this. PDR divides the path procedure into gait monitoring, step estimation and heading estimation [5], which has a relatively mature correlation for each process. Algorithm [6] makes PDR have very high positioning accuracy in a short time. However, there are two obvious problems in PDR. One is that the PDR needs the externally given initial value, and the other is that the integral deviation of the gyroscope will cause the cumulative error of the PDR. If the cumulative error is not externally corrected, the positioning result will be completely unavailable. Therefore, under these conditions, the combination of PDD and PDR can make up for the defects of the respective systems.

Section II introduces the pseudorange double difference model and PDR technology. The third section gives the fusion algorithm model in details, and the data analysis and corresponding processing methods are carried out for the problems of mobile phone implementation. The fourth section implements the algorithm and the experiments was carried out to verify it. The performance of the fusion algorithm is finally given.

2 PDD and PDR Model

2.1 PDD Model

The paper detailed the methods to assemble the data into RINEX format files through the original measurement of the mobile phone obtained by the API (Application Programming Interface) of the Android system, as well as obtaining the pseudorange and Doppler observation. After that, the pseudorange and doppler values can be effectively fetched from smartphone.

The pseudorange and doppler observation equations are as follows:

$$\rho_u^{(n)} = r_u^{(n)} + \delta t_u - \delta t^{(n)} + I_u^n + T_u^n + \xi_{\rho u}^{(n)} \quad (1)$$

$$\dot{\rho}_u^{(n)} - v^{(n)} \cdot 1_u + \delta f^{(n)} - \xi_{\rho u}^{(n)} = -v_u \cdot 1_u + \delta f_u \quad (2)$$

Where the superscript n represents the satellite number, ρ represents the pseudorange observation of the mobile phone obtained from the difference between the transmission time and the reception time, r means the true distance from the satellite to the user, I and T separately represent the ionosphere and troposphere errors, ξ denotes the other errors in the pseudorange measurement, f describes the frequency drift in the Doppler observation, 1 represents the unit vector from the satellite pointing to the user, and v represents the speed of the user's satellite.

If traditional Kalman filter is directly adopted, the nonlinear system needs to introduce an Extended Kalman Filter (EKF) for linearization. Meanwhile, the ionosphere and troposphere may produce tens of meters of error. In previous studies [4], it was also pointed out that the mobile phone GNSS clock has strong instability and might generate intermittent clock drift. Therefore, we eliminate or attenuate the above error term by the pseudorange double difference equation. In the pseudorange double difference system, $\boldsymbol{I}_r = \boldsymbol{I}_u$ based on the short baseline assumption, which means baseline is less than 10 km, thus $r_{ur} = -b_{ur} \cdot l_r$. The baseline vector 1 is no longer acquired by the mobile phone, thus making the mobile phone the relationship of speed and position are decoupled, and the original nonlinear system also becomes a linear system. Therefore, the traditional Kalman filter can be applied. As a cost, assuming that the noise of the double-difference model is Gaussian noise, the system noise will be twice the original noise variance along with the difference process. Moreover, a minimum of five visible and effective satellites are essential for differential positioning.

Observation process of pseudorange double difference system:

$$\begin{bmatrix} \rho_{ur}^{1} - \rho_{ur}^{j} \\ \rho_{ur}^{2} - \rho_{ur}^{j} \\ \cdots \\ \rho_{ur}^{i} - \rho_{ur}^{j} \end{bmatrix} = \begin{bmatrix} -\left[I_r^{(1)} - I_r^{(j)} \right] \cdot v_u \\ -\left[I_r^{(2)} - I_r^{(j)} \right] \cdot v_u \\ \cdots \\ -\left[I_r^{(i)} - I_r^{(j)} \right] \cdot v_u \end{bmatrix}$$

$$\begin{bmatrix} \rho_{ur}^{1} - \rho_{ur}^{j} \\ \rho_{ur}^{2} - \rho_{ur}^{j} \\ \cdots \\ \rho_{ur}^{i} - \rho_{ur}^{j} \end{bmatrix} = \begin{bmatrix} -\left[I_r^{(1)} - I_r^{(j)} \right] \cdot b_{ur} \\ -\left[I_r^{(2)} - I_r^{(j)} \right] \cdot b_{ur} \\ \cdots \\ -\left[I_r^{(i)} - I_r^{(j)} \right] \cdot b_{ur} \end{bmatrix} \tag{3}$$

$$K = P_k C^T (C P_k C^T + R)^{-1}$$

Where ρ_{ur} is the user pseudorange observation minus the base pseudorange value, K is the gain matrix, R is the observed noise matrix, and C denotes the relationship matrix between the observation vector and the state vector.
Prediction process:

$$\begin{bmatrix} \mathrm{b_{ur}} \\ \mathrm{v} \end{bmatrix} = \begin{bmatrix} 1 & \mathrm{T_S} \\ 0 & 1 \end{bmatrix} \begin{bmatrix} \mathrm{b_{ur}} \\ \mathrm{v} \end{bmatrix} \tag{4}$$

Where bur represents the baseline vector of the user to the base station and v represents the user speed.

2.2 PDR Model

The traditional PDR algorithm is based on the IMU bundled on the pedestrian's body for dead reckoning [7]. Since the IMU is fixed on the pedestrian's body, the inertial signal collected by the inertial sensor can accurately reflect the pedestrian's motion, zero-speed correction (Zero velocity update (ZUPT) [8] method could obtain the accurate positioning position of pedestrians, but it would limit the walking mode of pedestrians in practical applications, besides it even brings inconvenience to pedestrians. Thus the PDR based on feet of pedestrians is unusefulness in practice. Therefore, the PDR algorithm for smartphones has been improved and supplemented accordingly.

Generally speaking, the PDR consists of three parts: (1) gait detection (2) compensation estimation (3) heading estimation. In this paper, the methods adopted in the three parts according to the MEMS characteristics of mobile phones are as follows:

Step1: Gait detection

The peak detection method [9] is adopted, that is, during the walking process of the pedestrian, the acceleration in the vertical direction changes drastically before and after the footsteps and then forms a signal peak. Monitoring the peak value of each period after setting the threshold, and the peak detection technique can judge the number of steps for pedestrians.

Step2: Step length estimation

The step length estimation is divided into empirical model [10], linear model [9], nonlinear model [11] and artificial intelligence model [12]. For convenience, we choose one of the linear models:

$$S = K \cdot \sqrt[4]{a_M - a_m} \quad (5)$$

Where K is the estimated parameter, which can be estimated by indoor training, a_M is the maximum value of vertical acceleration in one cycle, and a_m is the minimum value of vertical acceleration in one cycle.

Step3: Heading estimation

The heading estimation of PDR is divided into INS and SHS [6], where INS is a three dimension and SHS is a two dimension. The magnetometer is susceptible to interference, so we use 6-axis information. In this paper, Madgwick's algorithm [13] is adopted, the gyroscope was chosen as the main one and the accelerometer is corrected to obtain the heading estimation angle.

3 PDD-PDR Fusion Algorithm

3.1 Data Pre-processing

In order to accurately perform pedestrian gait detection, the acceleration signal actually acquired during walking is usually pre-processed before the above PDR algorithm is adopted. Since high frequency noise is present in the actually collected acceleration signal, the signal is de-noised by a low pass filter. In view of the pedestrian's step frequency characteristics, an equal-ripple FIR low-pass filter is designed to pre-filter the IMU data, and the cut-off frequency is set to 3HZ. After pre-filtering, considering that pedestrian walking is a low dynamic motion, in order to further smooth the result, the low-pass filtered data is selected as a valid value every three points, and polynomial interpolation is performed between the two effective values to recover.

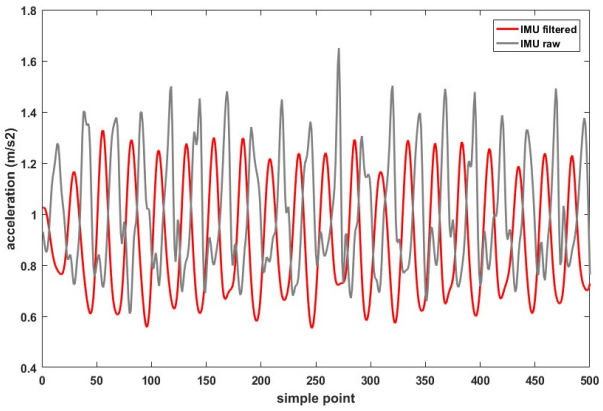

Fig. 1 Comparison of IMU pre- and post-processing data

As the above figure shows that, 5after pre-filtering and other processing, the IMU data is obviously smoothed and the mutation point is suppressed.

Since the GNSS positioning result curve is not smooth, in order to make the yaw angle calculated by the GNSS smoother, Kalman filtering is initially performed on the GNSS signal. On a account of the low rate of change of the walking attitude, the time delay caused by the two-stage filter is acceptable.

There are two ways to estimate yaw angles for GNSS, one estimation based on location [14]:

$$\varphi^{GNSS} = \arctan\left(\frac{\triangle P_k^{GNSS,E}}{\triangle P_k^{GNSS,N}}\right) \quad (6)$$

Where ΔP represents the displacement vector at step k, and E and N represent the direction.

Another estimation method is based on speed [15]:

$$\varphi^{GNSS} = \arctan\left(\frac{V_k^{GNSS,E}}{V_k^{GNSS,N}}\right) \quad (7)$$

Where v represents the velocity value of the Doppler shift of the k step.

In theory, the accuracy of satellite Doppler is much larger than the pseudorange accuracy and its velocity accuracy is also greater than the positional accuracy. For the position is obtained by Kalman filtering, the front and back positions have correlation while the Doppler value has no time correlation. This can also be illustrated in the experimental data analysis.

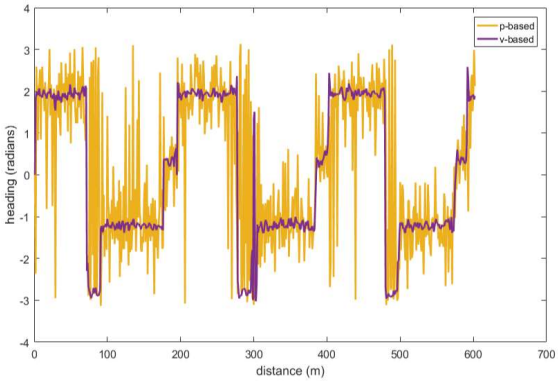

Fig. 2 Comparison of velocity-based and position-based estimation of yaw

As Fig.2 shows that, the yaw angle estimated based on the velocity value obtained by Doppler shift is significantly better than the yaw angle estimated by the position, so in the actual judgment we will adopt the speed-based yaw angle estimation method.

3.2 Fusion Algorithm

In view of the characteristics of PDR and GNSS, the path obtained by PDR has strong continuity, no breakpoints appear, and the heading estimation is highly reliable in a short time, while GNSS does not have cumulative error, but in a short time the characteristics of the larger error. This paper chooses the tight coupling of the two systems in the solution position, velocity and yaw angle estimation.

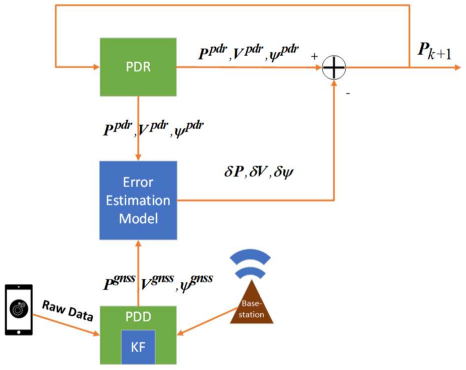

Fig. 3 PDD and GNSS fusion algorithm framework

The framework of the fusion algorithm is shown in Fig.3. The original measurement of the mobile phone and the observation of the base station firstly obtain the PDD positioning result through a Kalman filter, and the relevant data of the PDR will be sent to the error estimation model simultaneously, and the second-order Kalman filtering is performed to deal with the fusion data. Since the position estimation of the PDR is a Markov process, the next time position contains the accumulated error of the previous step. In addition, the update rate of PDR is higher than GNSS system which should be corrected higher-frequency. Therefore, the position correction value would be fed back to the PDR system as the initial value of the next moment. Compared with the non-feedback fusion system, the algorithm can correct the drift of PDR in real time, thus preventing the accumulated error caused by too long time. Among them, the heading of the PDR coincides with the Y axis of the mobile phone (API designation, directly above the screen), and the speed of the PDR is defined as the average speed within one step, which is obtained by the following formula:

$$\mathrm{v}_k^{PDR} = \frac{S_k}{t_k - t_{k-1}} \tag{8}$$

Where S represents the step size and t_k represents the time point of the k step.

The position estimate is obtained by the following formula:

$$\mathrm{E}_k = \mathrm{E}_{k-1} + \mathrm{S}_{k-1} \cdot \sin(\varphi_{k-1}) \tag{9}$$

$$\mathrm{N}_k = \mathrm{N}_{k-1} + \mathrm{S}_{k-1} \cdot \cos(\varphi_{k-1}) \tag{10}$$

Where E represents the position coordinate in the E direction in the ENU (East North Up) coordinate system, N represents the position coordinate in the north direction, and φ represents the yaw angle.

It should be noted that the position and velocity vectors obtained with pseudorange and Doppler are in the WGS84 world coordinate system, while the PDR is in the ENU coordinate system, so the GNSS positioning results need to be mapped to the ENU coordinate system.

PDR and GNSS error fusion observation process as follows :

$$\begin{bmatrix} \mathrm{W} \cdot \mathbf{P}^{\mathrm{GNSS}} - \mathbf{P}^{\mathrm{PDR}} \\ \mathrm{W} \cdot \mathbf{V}^{\mathrm{GNSS}} - \mathbf{V}^{\mathrm{PDR}} \\ \mathrm{W} \cdot \varphi^{\mathrm{GNSS}} - \varphi^{\mathrm{PDR}} \end{bmatrix} = \begin{bmatrix} \delta\mathbf{P} \\ \delta\mathbf{V} \\ \delta\varphi \end{bmatrix} \tag{11}$$

Where P represents the position vector, V represents the velocity vector, represents the yaw angle, and W is a weight function related to the carrier-to-noise ratio of the GNSS signal. This weighting is vital in the error model, because the error can be regard as the trustworthiness of the PDD and PDR errors, that is, the reliability degree of GNSS positioning accuracy. Since the GNSS error is not strictly obeying the Gaussian distribution, and the error model is filtered by KF, it can be considered that the credible subsystem we focused on depends on the CNR of GNSS. W is defined as:

$$\mathrm{W} = {\sum cnr_i}/{50n} \tag{12}$$

Where cnr_i represents the carrier-to-noise ratio of the i satellite used for positioning at this time, n represents the sum of the number of effective satellites used for positioning at this time, and 50 dB-Hz is the maximum CNR obtained from empirical values.

Forecasting process:

$$\begin{bmatrix} \delta \mathbf{P}_k \\ \delta \mathbf{V}_k \\ \delta \varphi_k \end{bmatrix} = \begin{bmatrix} 1 & \Delta t & 0 \\ 0 & 1 & 0 \\ 0 & 0 & 1 \end{bmatrix} \begin{bmatrix} \delta \mathbf{P}_{k-1} \\ \delta \mathbf{V}_{k-1} \\ \delta \varphi_{k-1} \end{bmatrix} \quad (13)$$

Where δP represents the positioning error of GNSS and PDR, which is used to correct the position deviation of PDR, and δV is used to correct the speed deviation of PDR, which is worth the time difference between step k and step k-1. The system noise is assumed to be Gaussian white noise, and the noise matrix is related to the noise power spectral density of the respective systems of PDD and PDR.

In theory, for system long-term running, GNSS also plays a role in correcting the step length estimator. At the same time, PDR reduces the dependence on differential system signal requirements. Although the Android API 24 provides an indicator for evaluating the reliability of GNSS data, we have set extra thresholds based on experience, such as setting the GNSS satellite elevation threshold to 15 degrees and the CNR threshold to 15 db. The threshold settings for other raw observations. See the literature [4]. Considering the limitations of the signal and the instability of the smartphone hardware, considering the signal error and the actual walking characteristics, it is determined that the signal is not available within the GNSS unit time (1s), that is, ||P_(x, y, k) - P_(x, y, k-1) |) | <400. In addition, the mobile phone GNSS chip has a low update rate of 1HZ, and the PDR has a time of <1s per step, so in fact, we will perform coarse time alignment by the timestamp alignment shown in the following figure, as shown in Figure 4. This will result in a time error of up to 1s.

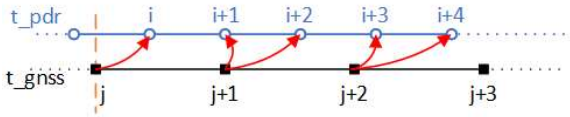

Fig. 4 Timestamp alignment of PDR and GNSS

4 EXPERIMENT ARCHITECTURE AND RESULT

4.1 Experiment architecture

The experimental platform is Huawei P10, the built-in GNSS chip is Broadcom BCM4774, the mobile phone IMU sampling frequency is 50HZ and the U-blox-

m8p equipped with South HYBLRB02R is tested for comparison experiments. The experimental test environment chose: (1) straight road with trees on both sides, (2) the loop route through two short tunnels (3) the loop road route under shade. The fusion positioning results will be mapped to Baidu Map.

4.2 Experiment results and analysis

All three test environments will give a comparison of the pseudorange double difference (PDD), pure PDR and PDR-PDD fusion algorithms. The path chose U-blox-m8p RTK mode result as ground truth. The real test scenarios are as follows:

(a) **(b)** **(c)**

Fig. 5 The photos of the three test scenarios

The picture (a) depicts the real scenario in photo, the road width is 10 meters and there are density trees on both sides. The open outdoor conditions on the middle line make the visible satellite number and signal quality enough to provide effective positioning results. Figure (b) shows the photo of the tunnel. The tunnel is not completely continuous which means weak GNSS signals could pass. Picture (c) shows the real scene of the tree-back loop. The road is two meters wide and the branches and leaves blind the light propagation, so the GNSS signal is blocked.

4.2.1 Open Road

In this section of the experiment, a straight road of 800 meters long is selected. During the walking stage, there are 5 stop points besides the beginning and end points.

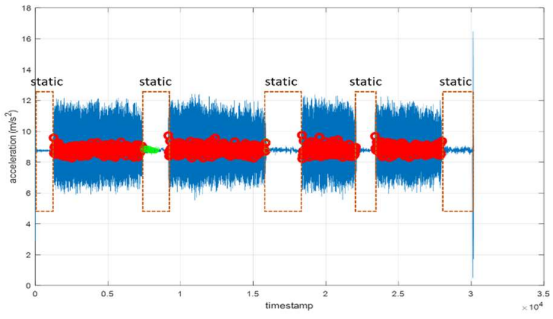

Fig. 6 The peak detection result of PDR

Above figure depicts the gait detection result. The detection diagram shows that the vibration and accelerometer method can clearly distinguish the accelerometer oscillation caused by pedestrian motion. The step detection is 757 steps and the actual walking is 757 steps. Thus success rate of step detection can achieve 100%.

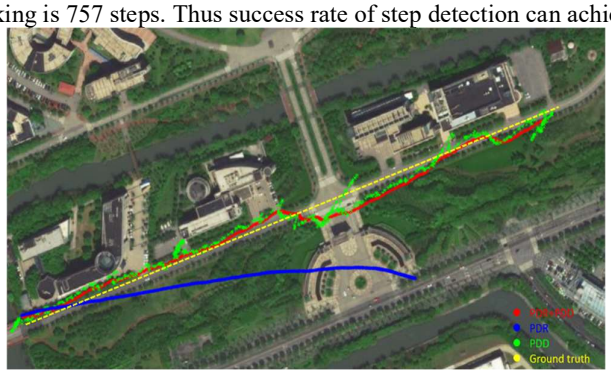

Fig. 7 The comparison results between PDR/PDD/PDR-PDD algorithms on open road

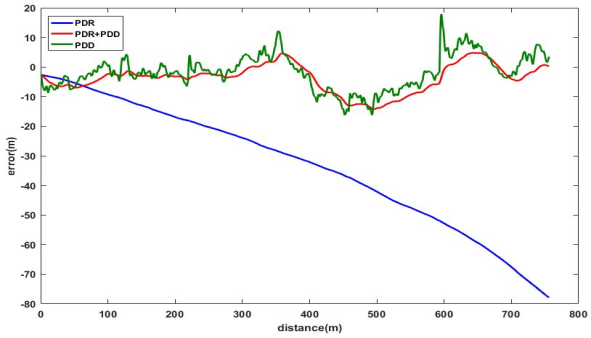

Fig. 8 The comparison curves of horizontal error

In the above figure, the standard deviation of PDD positioning error is 5.7 meters. It can be seen that the positioning results are obviously divergent at the five resting positions during the traveling, and there are some directions in a certain period. Large offset on specific segment indicating that trees and buildings on both sides of the road have a certain degree of multipath interference to the GNSS signals; the pure PDR positioning results have no divergence problems, and the positioning results are very smooth, but the problem is that the cumulative error of PDR leads to a rapid drift, and due to the inaccuracy of the initial value, the PDR is unable to return to the correct trajectory. However, the standard deviation of the positioning result of the PDR-PDD fusion algorithm is 3.3 meters, which keeps the smoothness and is not affected by the cumulative error of PDR, thus the result is always near the ground truth.

4.2.2 Tunnel Loop

The experimental site of this section selects a 1km long circular loop route. There are 65m and 40m short tunnels in the north and south sections of the route respectively. There is no stoppage during the whole route.

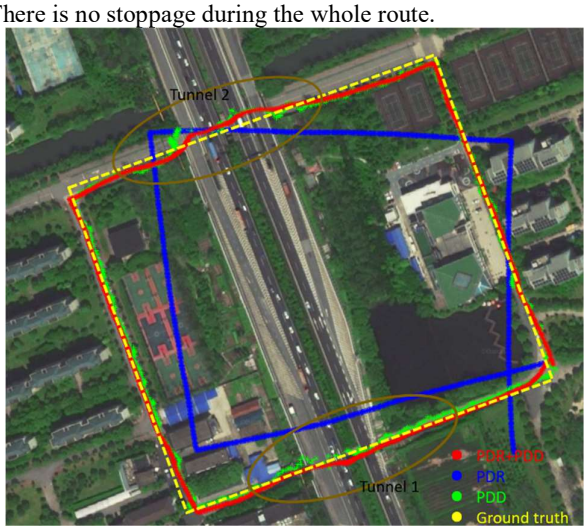

Fig. 9 The comparison results between PDR/PDD/PDR-PDD algorithms on tunnel loop

Compared with the first test on the open road, the PDD under continuous motion has no divergence point in case of good signal condition, and the positioning effect outside the tunnel is within 5 meters. However, when passing through the tunnel section, the positioning result is obviously divergent, and the density of positioning in the tunnel area is smaller than the normal environment. Due to the tunnel conditions, the PDD positioning point is mainly predicted by the position before entering the tunnel and the residual value of Doppler in the Kalman filter. In the pure PDR algorithm, the estimation error of the initial heading and the angle estimation of the two turns are estimated. The error occurs, which leads to a deviation of about 100 meters from the initial point of the loopback, and the positioning trajectory is quite different from the actual trajectory. At the same time, the positioning trajectory of the PDR-PDD algorithm has the same accuracy of GNSS in the tunnel-free region. In the two tunnel sections, the positioning trajectory is smooth and continuous, and the end point of the loopback and the starting point can be considered to be in the same position, indicating that the fusion algorithm is very effective.

4.2.3 Shade Loop

This test was executed in a rectangular loopback route under the shade of 840 meters. The long side of the route is 300 meters and the short side is 120 meters. There is no stopping point during the whole route.

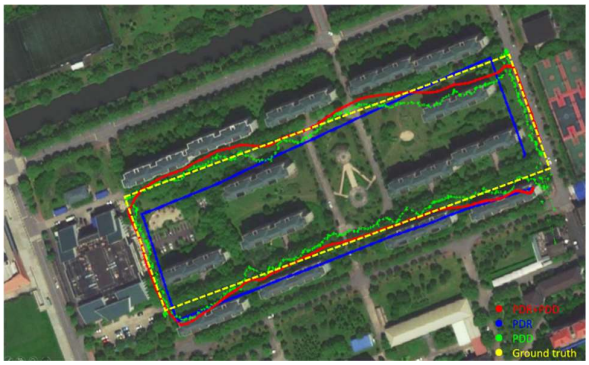

Fig. 10 The comparison results between PDR/PDD/PDR-PDD algorithms on shade loop

In the above figure, it can be seen that the blocking effect of the tree shade on the signal of GNSS has a great influence, and the error of PDD is greater than 10 meters, while the pure PDR algorithm accurately reflects the pedestrian rectangular trajectory, but due to the step length estimation PDR track is deflected ahead of the intersection; Meanwhile, the positioning result of the PDR-PDD fusion algorithm can roughly reflect the walking trajectory and the variance is small relative to PDD and PDR. The trajectory in the tunnel experiment still has a greater unsmoothing effect compared to the previous two tests. This is because the PDD performance is terrible, and there is still a large error in the smoothing process. In the PDD-PDR algorithm we purposed, if one of the systems has a poor quality, it will inevitably lead to a large deviation in the fusion result. Despite this, the PDD-PDR fusion algorithm is still superior to other algorithms.

Table 1. Algorithm results of different experiments

scenario	Error items	PDD	PDR	PDR-PDD
Open road	Mean(m)	4.8	45.2	4.5
	σ(m)	7.4	49	5.2
Tunnel loop	Mean(m)	7.1	71.5	3.2
	σ(m)	8.1	74.2	3.5
Shade loop	Mean(m)	16.2	21.3	8.8
	σ(m)	19.3	22.1	10.7

5 Conclusion

This paper proposes a PDR-PDD fusion algorithm based on smartphone, which initially realizes the high-precision positioning using the original GNSS observation

and built-in MEMS-IMU. According to the characteristics of the mobile phone device, the paper applies a targeted data processing. The pseudorange double difference result is filtered by the error model and the PDR system is synchronously corrected in real time, and the offset caused by the accumulated error is avoided by the feedback system. Experiments show that in the dynamic and static alternating motion, short-term signal loss and poor signal quality under the shade can achieve good positioning results, but at the same time, it is found that in the process of fusion, a large error point in subsystem would has a significant impact on the fusion result. In the future work, the signal reliability will be estimated in advance on the original observation to influence the weight of the PDD system, thus avoiding the interference of large error on the overall system.

1.3 References

[1] S. Banville and F. J. G. W. Diggelen, "Innovation: Precise positioning using raw GPS measurements from Android smartphones," 2016.

[2] K. M. Pesyna Jr, R. W. Heath Jr, and T. E. Humphreys, "Centimeter positioning with a smartphone-quality GNSS antenna," in Radionavigation Laboratory Conference Proceedings, 2014.

[3] T. E. Humphreys, M. Murrian, K. M. Pesyna Jr, S. Podshivalov, and F. van Diggelen, "On the feasibility of cm-accurate positioning via a smartphone's antenna and GNSS chip," in Radionavigation Laboratory Conference Proceedings, 2016.

[4] Z. Wu, Liu, Peilin, Liu, Qiang, Wang, Yuze, "MEMS-based IMU Assisted Real Time Difference Using Raw Measurements from Smartphone," Proceedings of the 31st International Technical Meeting of The Satellite Division of the Institute of Navigation (ION GNSS+ 2018), Miami, Florida, September 2018, pp. 445-454.

[5] J. Qian, J. Ma, R. Ying, P. Liu, and L. Pei, "An improved indoor localization method using smartphone inertial sensors," in Indoor Positioning and Indoor Navigation (IPIN), 2013 International Conference on, 2013, pp. 1-7: IEEE.

[6] R. J. I. C. S. Harle and Tutorials, "A survey of indoor inertial positioning systems for pedestrians," vol. 15, no. 3, pp. 1281-1293, 2013.

[7] T. Gadeke, J. Schmid, M. Zahnlecker, W. Stork, and K. D. Muller-Glaser, "Smartphone pedestrian navigation by foot-IMU sensor fusion," in Ubiquitous Positioning, Indoor Navigation, and Location Based Service (UPINLBS), 2012, 2012, pp. 1-8: IEEE.

[8] S. K. Park and Y. S. J. S. Suh, "A zero velocity detection algorithm using inertial sensors for pedestrian navigation systems," vol. 10, no. 10, pp. 9163-9178, 2010.

[9] R. W. Levi and T. Judd, "Dead reckoning navigational system using accelerometer to measure foot impacts," ed: Google Patents, 1996.

[10] R. Chen, L. Pei, and Y. Chen, "A smart phone based PDR solution for indoor navigation," in Proceedings of the 24th International Technical Meeting of the Satellite Division of the Institute of Navigation, 2011, pp. 1404-1408.

[11] D. Alvarez, R. C. González, A. López, and J. C. Alvarez, "Comparison of step length estimators from wearable accelerometer devices," in Encyclopedia of Healthcare Information Systems: IGI Global, 2008, pp. 244-250.

[12] S. Beauregard and H. Haas, "Pedestrian dead reckoning: A basis for personal positioning," in Proceedings of the 3rd Workshop on Positioning, Navigation and Communication, 2006, pp. 27-35.

[13] S. J. R. x.-i. Madgwick and U. o. Bristol, "An efficient orientation filter for inertial and inertial/magnetic sensor arrays," vol. 25, pp. 113-118, 2010.
[14] H. Lan, C. Yu, and N. El-Sheimy, "An integrated PDR/GNSS pedestrian navigation system," in China Satellite Navigation Conference (CSNC) 2015 Proceedings: Volume III, 2015, pp. 677-690: Springer.
[15] L.-T. Hsu, Y. Gu, Y. Huang, and S. J. I. S. J. Kamijo, "Urban pedestrian navigation using smartphone-based dead reckoning and 3-D map-aided GNSS," vol. 16, no. 5, pp. 1281-1293, 2016.